

DYNAMIC BEHAVIOR OF A PACED CARDIAC FIBER*

JOHN W. CAIN†

Abstract. Consider a typical experimental protocol in which one end of a one-dimensional fiber of cardiac tissue is periodically stimulated, or paced, resulting in a train of propagating action potentials. There is evidence that a sudden change in the pacing period can initiate abnormal cardiac rhythms. In this paper, we analyze how the fiber responds to such a change in a regime without arrhythmias. In particular, given a fiber length L and a tolerance η , we estimate the number of beats $N = N(\eta, L)$ required for the fiber to achieve approximate steady-state in the sense that spatial variation in the diastolic interval (DI) is bounded by η . We track spatial DI variation using an infinite sequence of linear integral equations which we derive from a standard kinematic model of wave propagation. The integral equations can be solved in terms of generalized Laguerre polynomials. We then estimate N by applying an asymptotic estimate for generalized Laguerre polynomials. We find that, for fiber lengths characteristic of cardiac tissue, it is often the case that N effectively exhibits no dependence on L . More exactly, (i) there is a critical fiber length L^* such that, if $L < L^*$, the convergence to steady-state is slowest at the pacing site, and (ii) often, L^* is substantially larger than the diameter of the whole heart.

Key words. cardiac fiber, pacing, transient behavior, restitution, kinematic model, generalized Laguerre polynomials

AMS subject classifications. 92C50, 33C45, 92C30

DOI. 10.1137/05063845X

1. Introduction. Cardiac cells have the property of *excitability*: when a stimulus current of sufficient strength is applied to a quiescent cell, the transmembrane voltage v undergoes a prolonged elevation, called an *action potential*, before eventually returning to its resting value. Repeatedly stimulated, or *paced*, cardiac cells exhibit sequences of action potentials. By specifying a threshold voltage $v = v_{\text{thr}}$, one may define the *action potential duration (APD)* as the amount of time in which $v > v_{\text{thr}}$ during an action potential. The recovery time during which $v < v_{\text{thr}}$ between successive action potentials is called the *diastolic interval (DI)*. As illustrated in Figure 1, we shall denote the APD following the n th stimulus by A_n and the subsequent DI by D_n .

Periodic pacing leads to one of several types of phase-locked responses depending on the underlying pacing period B . For large B , cells exhibit a 1:1 response in which every stimulus yields an identical action potential. For smaller B , one sometimes observes a period-2 response, known as *alternans*, in which APD and DI values exhibit beat-to-beat alternation [21, 23, 24, 28, 29]. If B is decreased even further, cells exhibit a 2:1 response in which only every other stimulus yields an action potential [15, 21, 35]. In what follows, we shall assume that all pacing periods are sufficiently large to ensure a 1:1 steady-state response.

In spatially extended tissue, neighboring cells are coupled electrically via gap junctions, allowing action potentials to propagate through the tissue [19, 25]. Below,

*Received by the editors August 19, 2005; accepted for publication (in revised form) May 1, 2006; published electronically July 31, 2006. The content of this article is adapted from the last chapter of the author's doctoral dissertation [3]. This work was supported by the National Science Foundation under grants DMS-9983320 and DMS-0244492 and the National Institutes of Health under grant 1R01-HL-72831.

<http://www.siam.org/journals/siap/66-5/63845.html>

†Department of Mathematics, Virginia Commonwealth University, Richmond, VA 23284-2014 (jwcain@vcu.edu).

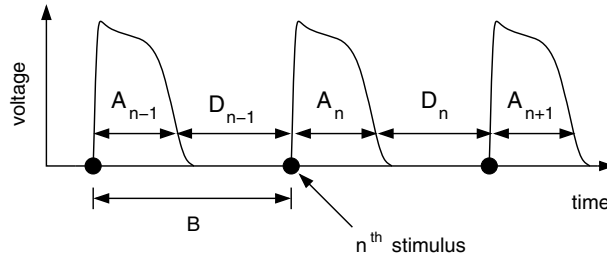


FIG. 1. Voltage trace of several action potentials in a paced cardiac cell.

we shall study the dynamics of a paced cardiac fiber composed of cylindrical cells joined together in an end-to-end fashion. We assume that voltage exhibits negligible radial dependence, varying only as a function of a length variable x ; that is, the fiber can be treated as one-dimensional. Moreover, we shall assume that pacing is performed at one end of the fiber which we identify with $x = 0$.

Typically, propagation of action potentials in a one-dimensional fiber is modeled using a reaction-diffusion equation known as the *cable equation*, which, after non-dimensionalization, takes the form

$$(1) \quad \frac{\partial v}{\partial t} = \frac{\partial^2 v}{\partial x^2} + g(v, w).$$

Here, $v = v(x, t)$ is the transmembrane voltage and w is a vector of various dynamic variables that are used in modeling the ionic mechanism of the action potential. For a derivation of the cable equation, see the texts of Plonsey and Barr [25] and Keener and Sneyd [19]. Examples of studies in which the cable equation is used to model cardiac dynamics include [5, 6, 7, 18, 22].

Although the cable equation serves as a popular model, we remark that arrhythmias, by nature, concern the *timing* of excitation and recovery of the cells. Therefore, it is often desirable to track the progress of propagating action potentials without regard to the structure of the voltage profile. Indeed, many recent studies [4, 8, 11, 12, 16, 30, 34] have employed *kinematic* models [19, 27] of wave propagation in cardiac fibers.

In this paper, we use a kinematic model to investigate how a fiber of length L responds to a sudden change in the pacing period, say from B_{old} to B_{new} . Changing the pacing period introduces spatial variation in APD and DI. Our primary goal is to estimate the number of beats required for the fiber to “adjust” to the new pacing period, i.e., the number of beats required to reach approximate steady-state in the sense that spatial variation in DI is small. No previous studies have analyzed the transient behavior following a change in the pacing period. In the course of solving our main problem, we shall provide such an analysis. Describing the persistence of spatial DI variation under such a pacing protocol may lead to an improved understanding of the mechanisms for initiation of arrhythmias such as discordant alternans [34].

To establish notation, refer to Figure 2, which illustrates both the spatial variation in DI induced by changing the pacing period from B_{old} to $B_{\text{new}} < B_{\text{old}}$ and the aforementioned convergence to a steady-state. Here, $D_n = D_n(x)$ denotes the n th DI following the change in the pacing period—in particular, $n = 1$ corresponds to the first beat with period B_{new} . Figure 2(a) shows $D_n(x)$ for $n = 1, \dots, 4$ and Figure 2(b) shows $D_n(x)$ for $n = 7, 8$. Note that $D_n(x)$ appears to converge pointwise to a constant

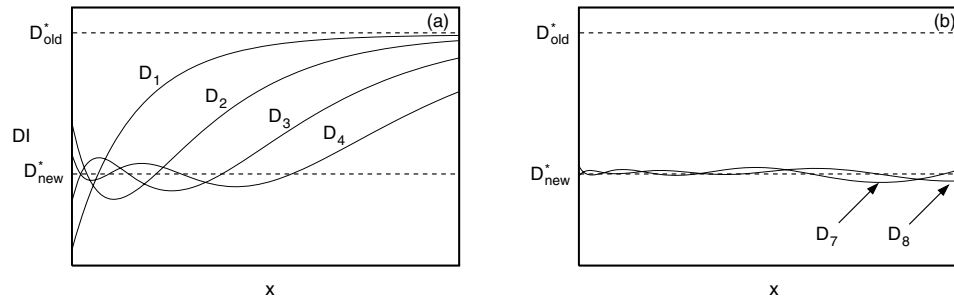


FIG. 2. Spatial variation in DI after changing the pacing period from B_{old} to $B_{new} < B_{old}$. (a) the curves $D_n(x)$ for $n = 1, \dots, 4$; (b) the curves $D_n(x)$ for $n = 7, 8$.

D_{new}^* as $n \rightarrow \infty$.

More quantitatively, our main problem may be stated as follows. Let $\eta > 0$ be a given tolerance, and let n and D_{new}^* be as in the preceding paragraph.

Goal: Estimate the number of beats $N = N(\eta, L)$ such that $|D_n(x) - D_{new}^*| < \eta$ for all $x \in [0, L]$, $n \geq N$.

Our analysis shows that, for fibers shorter than a critical length $L = L^*$, the convergence is slowest at the pacing site $x = 0$. In other words, $N(\eta, L)$ does not depend on the fiber length L provided that $L < L^*$. Moreover, we find that $L^* \rightarrow \infty$ as the slope of the restitution curve at $DI = D_{new}^*$ tends to 1. Hence, $N(\eta, L)$ is especially unlikely to exhibit any length dependence as we approach the bifurcation to alternans.

The remainder of this paper is organized as follows. In section 2, we recall a kinematic model [19, 27] of wave propagation, which allows us to follow the progress of each action potential without tracking the complete voltage profile $v(x, t)$. From the kinematic model, we derive a recursive sequence of linear equations which can be solved to yield approximations $y_n(x)$ of $D_n(x) - D_{new}^*$, allowing us to monitor the convergence to steady-state. As explained in section 3, the functions $y_n(x)$ can be expressed in terms of generalized Laguerre polynomials. The behavior of the functions $y_n(x)$ can be approximated by recalling a large- n asymptotic estimate for the generalized Laguerre polynomials. This allows us to estimate the maximum of $|y_n(x)|$ on the interval $[0, L]$, thereby leading to an estimate of $N(\eta, L)$. The estimate of $N(\eta, L)$ is given by one of two formulas according to whether $L < L^*$ or $L > L^*$. Section 4 contains a summary and discussion of our results.

2. Derivation of the governing equations. We begin this section with a brief discussion of the restitution and dispersion curves. We then recall a kinematic model of action potentials propagating in a paced fiber. From the equations of the kinematic model, we derive a sequence of linear equations which will allow us to solve the main problem.

2.1. Restitution and dispersion curves. Cardiac cells exhibit electrical *restitution*: The steady-state APD at a given pacing period B decreases as B is shortened. Nolasco and Dahlen [23] were among the first to model restitution with a mapping

$$(2) \quad A_{n+1} = f(D_n) = f(B - A_n).$$

Guevara et al. [14] later showed that alternans can result from a period-doubling bifurcation of (2) as the pacing period B is decreased. The function f is called the *restitution function*, and its graph is called the *restitution curve*. The restitution curve is typically monotone increasing; i.e., more recovery time yields longer excitations. Many authors (see, for example, [1, 2, 15]) have fit restitution data with exponential functions of the form

$$(3) \quad f(DI) = APD_{\max} - ke^{-DI/\tau},$$

where APD_{\max} , k , and τ are positive constants. We shall not specify a functional form for the restitution function but will assume that f has the same qualitative shape as (3).

Just as APD depends upon the preceding DI, the wave front velocity of an action potential in a fiber depends upon the preceding (local) DI. This dependence is often displayed graphically via the *dispersion curve*, which typically has the same qualitative shape as the restitution curve. We shall denote the functional form of the dispersion curve by $c(DI)$.

2.2. Kinematic model of wave propagation. To solve the problem of estimating $N(\eta, L)$, we need only track the progress of action potentials, not their complete structure. Hence, we shall employ a kinematic model of wave propagation [19, 27]. In doing so, we implicitly assume that recovery always occurs via a phase wave [9, 33]; i.e. the wave back of each action potential is not greatly affected by diffusion. We also adopt the following assumptions, the last two of which are specific to the pacing protocol described in the introduction:

- (A1) To a reasonable approximation, the tissue does not exhibit *memory*: As implicitly assumed in (2), A_{n+1} depends only upon D_n and is not greatly influenced by the past pacing history. Likewise, the wave front velocity of the $(n + 1)$ st action potential depends only upon $D_n(x)$, the preceding local DI.
- (A2) The restitution and dispersion curves are monotone increasing.
- (A3) To implement the pacing protocol outlined in the introduction, the interval between the n th and $(n + 1)$ st stimuli is B_{old} if $n \leq 0$ and B_{new} if $n > 0$.
- (A4) Prior to the change in the pacing period (i.e., for $n \leq 0$), the long-term pacing with period B_{old} leads to a 1:1 steady-state response in which DI is a constant,¹ say D_{old}^* . In particular, $D_0(x) \equiv D_{\text{old}}^*$.

We now recall how to use the information contained in the restitution and dispersion curves to track the wave fronts and wave backs of the action potentials. If we pace one end (say $x = 0$) of a fiber and plot $v(x, t)$ versus x and t , we obtain a surface in three-dimensional space. Taking the intersection of this surface with the plane $v = v_{\text{thr}}$, we generate a sequence of curves which we identify with the wave fronts and wave backs of the action potentials. Projecting these curves onto the xt plane yields a schematic space-time plot of the wave fronts and wave backs as illustrated in Figure 3. Here, $\phi_n(x)$ (resp., $\beta_n(x)$) denotes the time at which the n th wave front (resp., wave back) arrives at x , and

$$(4) \quad CL_n(x) = \phi_{n+1}(x) - \phi_n(x)$$

¹Referring to (2) with $B = B_{\text{old}}$, note that D_{old}^* is the unique DI satisfying the equation $DI + f(DI) = B_{\text{old}}$.

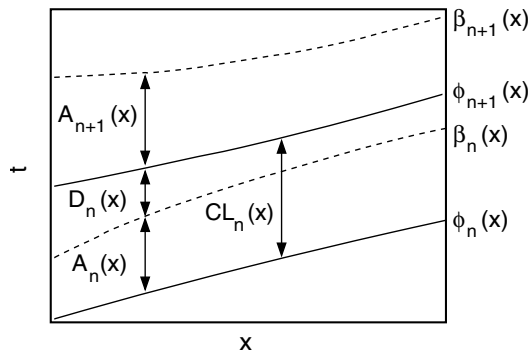


FIG. 3. Schematic diagram of wave fronts (solid curves) and wave backs (dashed curves).

is called the *cycle length*. Since

$$(5) \quad A_n(x) = \beta_n(x) - \phi_n(x) \quad \text{and} \quad D_n(x) = \phi_{n+1}(x) - \beta_n(x),$$

we may also express the cycle length as

$$(6) \quad CL_n(x) = A_n(x) + D_n(x).$$

From our assumption that recovery occurs via a phase wave, we may apply the restitution function locally at each x along the fiber:

$$(7) \quad A_n(x) = f(D_{n-1}(x)) \quad (0 \leq x \leq L).$$

The slope of $\phi_n(x)$ is related to the speed of the n th wave front:

$$(8) \quad \frac{d\phi_n}{dx} = \frac{1}{c(D_{n-1}(x))} \quad (0 < x < L).$$

By (6) and (7), the cycle length satisfies an algebraic condition

$$(9) \quad CL_n(x) = D_n(x) + f(D_{n-1}(x)),$$

and by (4) and (8), the cycle length also satisfies a differential equation

$$(10) \quad \frac{dCL_n}{dx} = \frac{1}{c(D_n(x))} - \frac{1}{c(D_{n-1}(x))}.$$

Combining (9) and (10), we obtain a sequence of differential equations involving only DI values:

$$(11) \quad \frac{d}{dx} [D_n(x) + f(D_{n-1}(x))] = G(D_n(x)) - G(D_{n-1}(x)),$$

where

$$(12) \quad G(DI) = \frac{1}{c(DI)}.$$

From assumption (A3) above, pacing at $x = 0$ yields the boundary condition

$$(13) \quad D_n(0) = \begin{cases} B_{\text{old}} - f(D_{n-1}(0)), & n \leq 0, \\ B_{\text{new}} - f(D_{n-1}(0)), & n > 0, \end{cases}$$

while assumption (A4) yields an initial condition

$$(14) \quad D_0(x) \equiv D_{\text{old}}^*.$$

Combining (11), (13), and (14), we obtain a sequence of equations that can be solved iteratively to determine $D_n(x)$ for $n > 0$ and $0 \leq x \leq L$.

2.3. Derivation of the main sequence of equations. To analyze the transient behavior following the change in the pacing period, we linearize (11), (13) for $n \geq 0$. The resulting sequence of initial value problems (see (16), (17)) leads to our main sequence of equations (see (23)), which we solve exactly in the next section to obtain approximations of the functions $D_n(x)$ for $n \geq 0$.

To linearize (11), (13) for $n \geq 0$, let D_{new}^* denote the steady-state DI associated with long-term pacing with period B_{new} and let $y_n(x)$ denote our approximation of $D_n(x) - D_{\text{new}}^*$. By (14), we have

$$(15) \quad y_0(x) = D_{\text{old}}^* - D_{\text{new}}^*,$$

a constant. For $n > 0$, the linearization of (11), (13) about D_{new}^* is given by

$$(16) \quad \frac{d}{dx} [y_n(x) + \alpha y_{n-1}(x)] = -\lambda [y_n(x) - y_{n-1}(x)],$$

$$(17) \quad y_n(0) = -\alpha y_{n-1}(0) \quad (n > 0),$$

where

$$(18) \quad \alpha = f'(D_{\text{new}}^*)$$

denotes the slope of the restitution curve evaluated at D_{new}^* and

$$(19) \quad -\lambda = G'(D_{\text{new}}^*).$$

The negative sign in (19) emphasizes that $G(DI) = 1/c(DI)$ is a monotone decreasing function, which follows from assumption (A2) in the previous subsection. We remark that

- α is dimensionless and λ has units of $(\text{length})^{-1}$;
- in the linearized dynamics, the rate of convergence to steady-state at the $x = 0$ boundary is determined by α , the Floquet multiplier [31] of the map $A_{n+1} = f(B_{\text{new}} - A_n)$.

Let us solve (16), (17) for $y_n(x)$ in terms of $y_{n-1}(x)$, resulting in a recursive sequence of equations. Rewriting (16) as

$$(20) \quad \frac{d}{dx} [y_n(x) + \alpha y_{n-1}(x)] = -\lambda [y_n(x) + \alpha y_{n-1}(x)] + (\alpha + 1)\lambda y_{n-1}(x),$$

we use $e^{\lambda x}$ as an integrating factor to obtain

$$(21) \quad \frac{d}{dx} \{e^{\lambda x} [y_n(x) + \alpha y_{n-1}(x)]\} = (\alpha + 1)\lambda e^{\lambda x} y_{n-1}(x).$$

Integration yields

$$(22) \quad e^{\lambda x} [y_n(x) + \alpha y_{n-1}(x)] = y_n(0) + \alpha y_{n-1}(0) + (\alpha + 1)\lambda \int_0^x e^{\lambda s} y_{n-1}(s) ds.$$

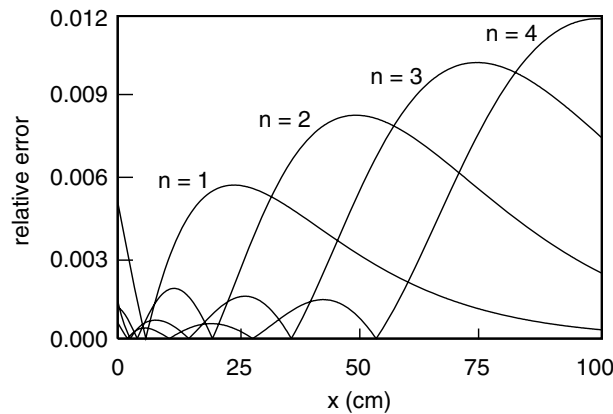


FIG. 4. Relative error in using $y_n(x)$ to approximate $D_n(x) - D_{\text{new}}^*$ for $n = 1, \dots, 4$.

Finally, applying boundary condition (17) and rearranging terms, we obtain our main sequence of equations,

$$(23) \quad y_n(x) = -\alpha y_{n-1}(x) + (\alpha + 1)\lambda \int_0^x e^{-\lambda(x-s)} y_{n-1}(s) ds \quad (n \geq 1).$$

Numerical evidence suggests that solutions of the linearized equations (23) exhibit good quantitative agreement with solutions of the original nonlinear equations (11) and (13). Figure 4 shows the relative error $|D_n(x) - D_{\text{new}}^* - y_n(x)|/D_n(x)$ versus x for $n = 1, \dots, 4$ after shortening the pacing period from $B_{\text{old}} = 340$ ms to $B_{\text{new}} = 320$ ms. The functions $D_n(x)$ were generated by numerical solution of (11) and (13) with f and c chosen as in (73) and (74), respectively. The functions $y_n(x)$ were generated by numerical solution of (23) with the same choices for f and c . We remark that these restitution and dispersion curves provide physiologically realistic APD values and propagation speeds for mammalian ventricular tissue [1, 13]. Note that the relative error (at least through four beats) never exceeds 0.012 even at the “un-physiological” distance of one meter from the stimulus site.

3. Estimating the rate of convergence to steady-state. Equation (23) allows us to determine y_n provided that y_{n-1} is known. In our case, $y_0(x)$ is a constant since $D_0(x) \equiv D_{\text{old}}^*$. We remark that, due to the simple form of $y_0(x)$, the recursive sequence of equations (23) can be solved exactly by successive substitutions. In doing so, it is advantageous to introduce some abstract notation (subsections 3.1 and 3.2) which helps us recognize that solutions of (23) can be expressed in terms of generalized Laguerre polynomials. Then, by applying a large- n asymptotic approximation of the Laguerre polynomials, we derive the desired estimate of $N(\eta, L)$ (see subsections 3.3 and 3.4).

3.1. Step 1: A Volterra integral operator. Motivated by (23), we define an operator $T = -\alpha I + (\alpha + 1)\lambda K$ on the Banach space $(C[0, L], \|\cdot\|_\infty)$, where I denotes the identity operator and

$$(24) \quad (K\psi)(x) = \int_0^x e^{-\lambda(x-s)} \psi(s) ds.$$

Then clearly $y_n = Ty_{n-1} = T^n y_0$. Our goal is to estimate the rate of convergence² of $y_n = T^n y_0$ to 0. To do so, we exploit the fact that y_0 is a constant function; i.e.,

$$(25) \quad \|T^n y_0\|_\infty = |y_0| \cdot \|T^n 1\|_\infty,$$

where y_0 is a constant. Our main problem can now be stated as

$$(26) \quad \text{Given any } \eta > 0, \text{ determine } N = N(\eta, L) \text{ such that} \\ \|T^n 1\|_\infty < \frac{\eta}{|y_0|} \text{ for all } n > N.$$

In the next subsection, we derive a formula for the function $(T^n 1)(x)$. Later, we will use asymptotics to learn more about the extrema of this function, using our results to estimate $\|T^n 1\|_\infty$.

3.2. Step 2: Computing powers of the operator T . Recalling that $T = -\alpha I + (\alpha + 1)\lambda K$, we may apply the binomial theorem to obtain

$$(27) \quad (T^m \varphi)(x) = \sum_{m=0}^n \binom{n}{m} (-\alpha)^{n-m} (\alpha + 1)^m \lambda^m (K^m \varphi)(x).$$

Powers of the operator K are straightforward to compute. For $m \geq 1$, we find that

$$(28) \quad (K^m \varphi)(x) = \int_0^x \int_0^{s_1} \dots \int_0^{s_{m-1}} e^{-\lambda(x-s_m)} \varphi(s_m) ds_m ds_{m-1} \dots ds_1.$$

Reversing the order of integration, the iterated integral (28) simplifies to a single integral

$$(29) \quad (K^m \varphi)(x) = \int_0^x \frac{(x-s_m)^{m-1}}{(m-1)!} e^{-\lambda(x-s_m)} \varphi(s_m) ds_m.$$

Combining (27) and (29) yields

$$(30) \quad (T^n \varphi)(x) = (-\alpha)^n \varphi(x) + \int_0^x \Psi_n(x-s) \varphi(s) ds = (-\alpha)^n \varphi(x) + \int_0^x \Psi_n(s) \varphi(x-s) ds,$$

where

$$(31) \quad \Psi_n(s) = e^{-\lambda s} \sum_{m=1}^n \binom{n}{m} (-\alpha)^{n-m} (\alpha + 1)^m \lambda^m \frac{s^{m-1}}{(m-1)!}.$$

It follows that

$$(32) \quad (T^n 1)(x) = (-\alpha)^n + \int_0^x \Psi_n(s) ds.$$

The functions Ψ_n can be expressed in terms of generalized Laguerre polynomials, a well-known class of special functions which can be defined as in the following definition (see Szegő [32]).

²We remark that the trivial estimate $\|y_n\|_\infty = \|T^n y_0\|_\infty \leq \|T\|^n \|y_0\|_\infty$ is too weak since $\|T\|$ can exceed 1. This is especially true close to the onset of alternans (i.e., as $\alpha \rightarrow 1^-$), in which case T is a contraction only for very short fiber lengths. However, it is straightforward [10, 26] to show that the spectral radius of T is simply α . Hence, if $\alpha < 1$, then $\|T^n y_0\|_\infty$ converges to 0 as $n \rightarrow \infty$.

DEFINITION 3.1. Let $\beta > -1$ and $n \geq 0$. Then the generalized Laguerre polynomial $L_n^{(\beta)}(x)$ is defined by

$$(33) \quad L_n^{(\beta)}(x) = \sum_{m=0}^n \binom{n+\beta}{n-m} \frac{(-x)^m}{m!}.$$

Comparing (31) and (33) with $\beta = 1$, it is straightforward to verify that

$$(34) \quad \Psi_n(s) = (-\alpha)^{n-1}(\alpha+1)\lambda e^{-\lambda s} L_{n-1}^{(1)}\left(\frac{\lambda(\alpha+1)s}{\alpha}\right).$$

By (32) and (34), we have

$$(35) \quad \begin{aligned} (T^n 1)(x) &= (-\alpha)^n + (-\alpha)^{n-1}(\alpha+1)\lambda \int_0^x e^{-\lambda s} L_{n-1}^{(1)}\left(\frac{\lambda(\alpha+1)s}{\alpha}\right) ds \\ &= (-\alpha)^n \left(1 - \int_0^{\frac{\lambda(\alpha+1)x}{\alpha}} e^{-\frac{\alpha s}{\alpha+1}} L_{n-1}^{(1)}(s) ds\right). \end{aligned}$$

3.3. Step 3: Large- n asymptotic estimate of $\|T^n 1\|_\infty$. In order to estimate $\|T^n 1\|_\infty$, we must approximate the integral in (35). To do so, we will make use of an asymptotic estimate for the generalized Laguerre polynomials. However, because the estimate we will use is not uniformly valid throughout the region of integration, we will split the region of integration into two subregions.

The following asymptotic approximation as $n \rightarrow \infty$ for the generalized Laguerre polynomials appears in Szegő [32, p. 199].

THEOREM 3.2. Let $\beta > -1$ and $n \rightarrow \infty$. Then

$$(36) \quad L_n^{(\beta)}(x) = \pi^{-\frac{1}{2}} e^{\frac{x}{2}} x^{-\frac{\beta}{2}-\frac{1}{4}} n^{\frac{\beta}{2}-\frac{1}{4}} \left[\cos\left(\sqrt{4nx} - \frac{\beta\pi}{2} - \frac{\pi}{4}\right) + (nx)^{-\frac{1}{2}} O(1) \right].$$

Moreover, given positive constants c and ω , the error term holds uniformly on the interval $cn^{-1} \leq x \leq \omega$.

Because the asymptotic approximation given by Theorem 3.2 breaks down for x small, we estimate (35) by splitting the interval of integration into two subintervals. For the boundary between the two subintervals, we use an approximation of the first root of $L_{n-1}^{(1)}$. Setting $\beta = 1$, note that the first two zeros of the approximation given by (36) occur when the argument of the cosine term is $-\pi/2$ or $\pi/2$. The $(nx)^{-1/2}$ error term influences the location of the first zero of (36) because it is not negligible for $x = O(1/n)$. Figure 5 suggests that we may approximate³ the first root of $L_n^{(1)}(x)$ as the value of x for which the cosine term in (36) is $\pi/2$, not $-\pi/2$. That is, $x = C/n$, where

$$(37) \quad C = \frac{25\pi^2}{64} = 3.8553\dots$$

In what follows, we will use $C/(n-1)$ as the boundary between the two subintervals of integration.

³A more precise estimate of $x_{1n}^{(\beta)}$, the first root of $L_n^{(\beta)}(x)$, appears in Szegő [32]: $\lim_{n \rightarrow \infty} (n x_{1n}^{(\beta)}) = (j_1^{(\beta)}/2)^2 = 3.6705\dots$, where $j_1^{(\beta)} = 3.8317\dots$ denotes the first positive zero of the Bessel function $J_\beta(x)$.

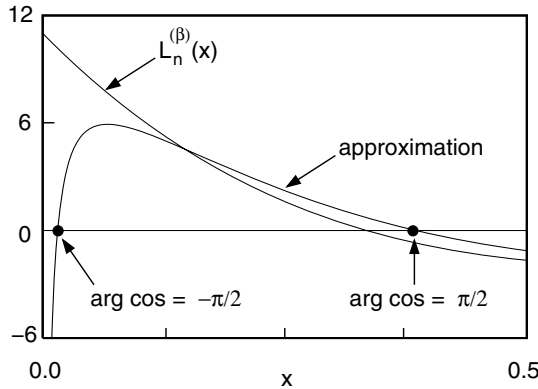


FIG. 5. Comparison of the generalized Laguerre polynomial $L_n^{(\beta)}(x)$ with the approximation given by Theorem 3.2 for $n = 10$ and $\beta = 1$. As indicated in the figure, the first two roots of the approximation (36) occur when the argument of the cosine function is $-\pi/2$ or $\pi/2$.

To estimate the integral in (35), we write

$$(38) \quad \int_0^{\frac{\lambda(\alpha+1)x}{\alpha}} e^{-\frac{\alpha s}{\alpha+1}} L_{n-1}^{(1)}(s) ds = \underbrace{\int_0^{\frac{C}{n-1}} e^{-\frac{\alpha s}{\alpha+1}} L_{n-1}^{(1)}(s) ds}_{\mathbf{I}_1} + \underbrace{\int_{\frac{C}{n-1}}^{\frac{\lambda(\alpha+1)x}{\alpha}} e^{-\frac{\alpha s}{\alpha+1}} L_{n-1}^{(1)}(s) ds}_{\mathbf{I}_2}.$$

Our expression for $(T^n 1)(x)$ now reads

$$(39) \quad (T^n 1)(x) = (-\alpha)^n (1 - \mathbf{I}_1 - \mathbf{I}_2).$$

Estimating \mathbf{I}_1 . To estimate the integral \mathbf{I}_1 in (38), we treat the two factors in the integrand separately. The factor $L_{n-1}^{(1)}(s)$ can be approximated by a quadratic function $q_{n-1}(s)$ by matching $L_{n-1}^{(1)}(s)$ and its derivative at $s = 0$ and using the fact that $L_{n-1}^{(1)}(C/(n-1)) \approx 0$. By algebra, we find that the polynomial

$$(40) \quad q_{n-1}(s) = \frac{n(n-1)^2}{C^2} \left(\frac{C}{2} - 1 \right) s^2 - \frac{1}{2} n(n-1)s + n$$

approximates the function $L_{n-1}^{(1)}(s)$ in the interval $[0, C/(n-1)]$. Because the exponential factor in the integrand of \mathbf{I}_1 is $1 + O(1/n)$ throughout the region of integration, we neglect this factor and compute

$$(41) \quad \mathbf{I}_1 \approx \int_0^{\frac{C}{n-1}} q_{n-1}(s) ds = \frac{2C}{3} - \frac{C^2}{12} + O\left(\frac{1}{n}\right).$$

In what follows, we will approximate \mathbf{I}_1 by

$$(42) \quad \mathbf{I}_1 \approx \frac{2C}{3} - \frac{C^2}{12} = 1.3315\dots$$

Estimating \mathbf{I}_2 . Integral \mathbf{I}_2 in (38) can be approximated by applying Theorem 3.2 with $\beta = 1$. Setting

$$(43) \quad \gamma = \frac{1 - \alpha}{2(1 + \alpha)},$$

we have

$$(44) \quad \mathbf{I}_2 \approx \pi^{-\frac{1}{2}}(n-1)^{\frac{1}{4}} \int_{\frac{C}{n-1}}^{\frac{\lambda(\alpha+1)x}{\alpha}} s^{-\frac{3}{4}} e^{\gamma s} \cos\left(\sqrt{4(n-1)s} - \frac{3\pi}{4}\right) ds.$$

Upon substituting $s \mapsto \sqrt{s}$, (44) becomes

$$(45) \quad \mathbf{I}_2 \approx 2\pi^{-\frac{1}{2}}(n-1)^{\frac{1}{4}} \int_{\sqrt{\frac{C}{n-1}}}^{\sqrt{\frac{\lambda(\alpha+1)x}{\alpha}}} s^{-\frac{1}{2}} e^{\gamma s^2} \cos\left(\sqrt{4(n-1)} \cdot s - \frac{3\pi}{4}\right) ds.$$

Integrating (45) by parts,

$$(46) \quad \begin{aligned} \mathbf{I}_2 \approx & \frac{s^{-\frac{1}{2}} e^{\gamma s^2} \sin\left(\sqrt{4(n-1)} \cdot s - \frac{3\pi}{4}\right)}{\sqrt{\pi}(n-1)^{\frac{1}{4}}} \Bigg|_{\sqrt{\frac{C}{n-1}}}^{\sqrt{\frac{\lambda(\alpha+1)x}{\alpha}}} \\ & - \frac{1}{\sqrt{\pi}(n-1)^{\frac{1}{4}}} \int_{\sqrt{\frac{C}{n-1}}}^{\sqrt{\frac{\lambda(\alpha+1)x}{\alpha}}} \left(-\frac{1}{2}s^{-\frac{3}{2}} + 2\gamma s^{\frac{1}{2}}\right) e^{\gamma s^2} \sin\left(\sqrt{4(n-1)} \cdot s - \frac{3\pi}{4}\right) ds. \end{aligned}$$

At first, the two terms in (46) appear to be of the same order, namely $O(n^{-1/4})$. However, for large n the rapid oscillation of the integrand of the volume term leads to cancellation, and hence the volume term is small relative to the boundary term. (This can also be seen by integrating by parts a second time.) Thus, we approximate \mathbf{I}_2 by retaining only the boundary terms in (46):

$$(47) \quad \begin{aligned} \mathbf{I}_2 \approx & \frac{u(x)}{(n-1)^{\frac{1}{4}}} \sin\left(\sqrt{\frac{4\lambda(\alpha+1)(n-1)x}{\alpha}} - \frac{3\pi}{4}\right) \\ & - \left(\frac{1}{C\pi^2}\right)^{\frac{1}{4}} e^{\frac{C(1-\alpha)}{2(1+\alpha)(n-1)}} \sin\left(\sqrt{4C} - \frac{3\pi}{4}\right), \end{aligned}$$

where

$$(48) \quad u(x) = \left(\frac{\alpha}{\pi^2\lambda(\alpha+1)x}\right)^{\frac{1}{4}} e^{\frac{\lambda(1-\alpha)x}{2\alpha}}.$$

The first term in (47) is bounded by

$$(49) \quad \frac{u(x)}{(n-1)^{\frac{1}{4}}},$$

and, for large n , the second term of (47) is approximately

$$(50) \quad \left(\frac{1}{C\pi^2}\right)^{\frac{1}{4}} \sin\left(\sqrt{4C} - \frac{3\pi}{4}\right) = \left(\frac{1}{C\pi^2}\right)^{\frac{1}{4}} = 0.4026\dots$$

By (39), (42), (49), and (50), we obtain the following approximate upper bound for $|(T^n \mathbf{1})(x)|$:

$$(51) \quad \begin{aligned} |(T^n \mathbf{1})(x)| & \lesssim \alpha^n \left| 1 - 1.3315 + 0.4026 + \frac{u(x)}{(n-1)^{\frac{1}{4}}} \right| \\ & = \alpha^n \left(0.0711 + \frac{u(x)}{(n-1)^{\frac{1}{4}}} \right) \quad (n \rightarrow \infty). \end{aligned}$$

3.4. Step 4: Estimates for $N(\eta, L)$. Referring to the definition (48) of $u(x)$, note that the $x^{-1/4}$ factor is dominant for small x while the exponential factor is dominant for large x . Hence, we expect $u(x)$ to have a single extremum—a global minimum. Letting L^* denote the x value at which the global minimum of $u(x)$ is attained (see (53) below), we are led to consider two cases when estimating $N(\eta, L)$: the case $L < L^*$ and the case $L > L^*$. In the former case, we shall demonstrate that $|(T^n 1)(x)|$ is always maximal at $x = 0$, indicating that the convergence to steady-state is slowest at the pacing site. In the latter case, $|(T^n 1)(x)|$ is maximal either at $x = 0$ or near $x = L$.

To determine L^* , we differentiate $u(x)$ with respect to x :

$$(52) \quad u'(x) = \left(\frac{\alpha}{\pi^2 \lambda (\alpha + 1)} \right)^{\frac{1}{4}} e^{\frac{\lambda(1-\alpha)x}{2\alpha}} \left(-\frac{1}{4} x^{-\frac{5}{4}} + \frac{\lambda(1-\alpha)}{2\alpha} x^{-\frac{1}{4}} \right).$$

The unique x value for which $u'(x)$ has a root is

$$(53) \quad L^* = \frac{\alpha}{2\lambda(1-\alpha)}.$$

With the above considerations in mind, we now derive our estimates for $N(\eta, L)$.

Case 1. $L < L^$.* From our preceding remarks, we see that the function $(T^n 1)(x)$ exhibits damped oscillatory behavior for $x < L^*$. Hence, $|(T^n 1)(x)|$ is maximal either at $x = 0$ or at the first local extremum of $(T^n 1)(x)$. In fact, we shall see that $|(T^n 1)(x)|$ is always maximal at $x = 0$.

PROPOSITION 3.3. *Let $x_{1(n-1)}^{(1)}$ denote the first root of $L_{n-1}^{(1)}(x)$. Then the first local extremum of $(T^n 1)(x)$ occurs at*

$$(54) \quad x_{\text{ext}} = \frac{\alpha}{\lambda(\alpha + 1)} x_{1(n-1)}^{(1)} \approx \frac{\alpha}{\lambda(\alpha + 1)} \cdot \frac{C}{n - 1}.$$

Proof. Differentiating (32) with respect to x , we obtain

$$(55) \quad (T^n 1)'(x) = \Psi_n(x) = (-\alpha)^{n-1} (\alpha + 1) \lambda e^{-\lambda x} L_{n-1}^{(1)} \left(\frac{\lambda(\alpha + 1)x}{\alpha} \right).$$

The only factor in (55) that can change sign as x varies is $L_{n-1}^{(1)}$. Hence, the first sign change of $\Psi_n(x)$ occurs when the $L_{n-1}^{(1)}$ factor has its first root, which occurs at $x = x_{\text{ext}}$. This x value corresponds to the first local extremum of $(T^n 1)(x)$. \square

Equation (35) gives the exact value of $|(T^n 1)(x)|$ at the $x = 0$ boundary, namely

$$(56) \quad |(T^n 1)(0)| = \alpha^n.$$

To estimate the value of $(T^n 1)(x)$ at its first local extremum, we refer to (51) and (54). By (54), we obtain the approximation

$$(57) \quad \frac{u(x_{\text{ext}})}{(n - 1)^{\frac{1}{4}}} \rightarrow \left(\frac{1}{C\pi^2} \right)^{\frac{1}{4}} \approx 0.4026 \quad (n \rightarrow \infty),$$

and (51) yields

$$(58) \quad |(T^n 1)(x_{\text{ext}})| \lesssim (0.0711 + 0.4026) \alpha^n \quad (n \rightarrow \infty).$$

Note that the coefficient of α^n in (58) is less than 1. Therefore, if $L < L^*$, we conclude that the convergence to steady-state is slowest at the $x = 0$ boundary. That is,

$$(59) \quad \|T^n 1\|_\infty = |(T^n 1)(0)| = \alpha^n.$$

With η and y_0 as in (26), we can now estimate the number of beats required to reach approximate steady-state:

$$(60) \quad N_1 = N_1(\eta) = \frac{\ln(\eta) - \ln|y_0|}{\ln(\alpha)}.$$

The subscript on N emphasizes that we presently consider the first case, $L < L^*$. Note that N_1 does not depend upon L , and the convergence to steady-state is slowest at the pacing site, $x = 0$.

Case 2. $L > L^$.* In this case, the function $u(x)$ may achieve its maximum at the right boundary of the interval $[C/(n - 1), L]$. By (51),

$$(61) \quad |(T^n 1)(L)| \lesssim \alpha^n \left(0.0711 + \frac{u(L)}{(n - 1)^{\frac{1}{4}}} \right) \quad (n \rightarrow \infty).$$

We wish to determine $N(\eta, L)$ such that

$$(62) \quad \alpha^n \left(0.0711 + \frac{u(L)}{(n - 1)^{\frac{1}{4}}} \right) < \frac{\eta}{|y_0|} \quad (\text{for all } n > N).$$

Taking logarithms and dividing through by $\ln \alpha$, we obtain

$$(63) \quad n + \frac{\ln \left(0.0711 + u(L)(n - 1)^{-\frac{1}{4}} \right)}{\ln \alpha} > N_1,$$

where N_1 is given by (60) above. Motivated by inequality (63), we define the function

$$(64) \quad g(n) = n + \frac{\ln \left(0.0711 + u(L)(n - 1)^{-\frac{1}{4}} \right)}{\ln \alpha} - N_1$$

and estimate the value of n for which $g(n)$ has a root. Because N_1 is large if $\eta/|y_0| \ll 1$, we use it as an initial guess and calculate

$$(65) \quad g(N_1) = \frac{\ln \left(0.0711 + u(L)(N_1 - 1)^{-\frac{1}{4}} \right)}{\ln \alpha}.$$

An improved estimate for the root of $g(n)$ is then given by

$$(66) \quad N_1 - g(N_1) = N_1 - \frac{\ln \left(0.0711 + u(L)(N_1 - 1)^{-\frac{1}{4}} \right)}{\ln \alpha}.$$

Comparing (66) with the expression (60), we obtain the desired estimate for $N(\eta, L)$ by taking the maximum of these two expressions:

$$(67) \quad N(\eta, L) = N_1 - \left[\frac{\ln \left(0.0711 + u(L)(N_1 - 1)^{-\frac{1}{4}} \right)}{\ln \alpha} \right]_+,$$

where

$$(68) \quad [a]_+ = \begin{cases} a, & a > 0, \\ 0 & \text{otherwise.} \end{cases}$$

In summary, the above approximations demonstrate that $|y_n(x)| = |y_0| \cdot |(T^n 1)(x)|$ is maximal near the boundaries of the interval $[0, L]$. The location of the maximum of $|(T^n 1)(x)|$ depends in part on whether the fiber length L exceeds a critical value L^* . The function $(T^n 1)(x)$ exhibits damped oscillatory behavior for $x < L^*$. Hence, if $L < L^*$, we conclude that $|(T^n 1)(x)|$ is maximal either at $x = 0$ or at the first local extremum of the function $(T^n 1)(x)$. Our computations rule out the latter case, and we find that $|(T^n 1)(x)|$ is always maximal at $x = 0$ if $L < L^*$. For $x > L^*$, the function $(T^n 1)(x)$ exhibits oscillations of growing amplitude and, in the worst case scenario, $|(T^n 1)(x)|$ is maximal at $x = L$. Our estimate of $N(\eta, L)$ is given by either (60) or (67) depending on whether L exceeds L^* .

A discussion of the physiological interpretation of the above results is provided in the next section.

4. Discussion and conclusions. We have described how a paced cardiac fiber responds when the pacing period is suddenly changed from B_{old} to B_{new} , providing the first analysis of the transient behavior resulting from such a pacing protocol. We estimated the number of beats $N(\eta, L)$ required for the spatial variation in DI to be small in the sense that

$$|D_n(x) - D_{\text{new}}^*| < \eta \quad \text{for all } x \in [0, L], \quad \text{for all } n \geq N.$$

The estimate is given by either (60) or (67) depending on whether the fiber length exceeds the critical value L^* defined by (53). According to our approximations, for $L < L^*$, the convergence to steady-state is slowest at the pacing site and the rate of convergence is determined by the slope α of the restitution curve evaluated at D_{new}^* .

To test these predictions, we performed numerical simulations of (11), (13), and (14) for a range of parameter values. In particular, we used the restitution and dispersion curves in the appendix (see (73), (74)), varying the parameters (69) within physiologically reasonable regimes for the mammalian ventricular action potential [1, 13] (e.g., peak conduction velocity of 60 ± 20 cm/sec). We also repeated the numerical simulations using simple exponential restitution and dispersion curves (see (3)), again for a range of parameter values. As expected, for short fiber lengths ($L < L^*$) the convergence is always slowest at the pacing site, and the transient lasts much longer as $\alpha \rightarrow 1^-$. Moreover, the estimate of $N(\eta, L)$ given by (60) typically provides a very accurate estimate (within several beats) of the actual number of beats required to achieve approximate steady-state. Not surprisingly, the estimate given by (60) breaks down if $|B_{\text{old}} - B_{\text{new}}|$ is large (on the order of hundreds of milliseconds) or if α is very close to 1.

For long fibers ($L > L^*$), the spatial DI profiles generated by numerical simulations are qualitatively similar to those shown in Figure 2(a)—in particular, the convergence $D_n(x) \rightarrow D_{\text{new}}^*$ is slowest at the far end of the fiber. In this case, (67) typically provides an accurate estimate of $N(\eta, L)$, with the same notable exceptions as in the case of short fibers (see preceding paragraph).

We remark that L^* is often so large that fibers of length $L > L^*$ are unrealistically long—on the order of tens of centimeters or even meters. For example, consider the restitution and dispersion curves in the appendix with parameter values given by (69).

Using $B_{\text{new}} = 266$ ms, one computes that $\alpha = 0.900$ and $\lambda = 0.127 \text{ cm}^{-1}$, which by (53) yields a critical fiber length L^* in excess of 35 cm. Equation (53) suggests that the critical length blows up as we approach the bifurcation to alternans: $L^* \rightarrow \infty$ as the slope $\alpha = f'(D_{\text{new}}^*) \rightarrow 1^-$, a prediction consistent with all of our numerical simulations. Therefore, N is especially unlikely to exhibit any length dependence if we are pacing in a regime close to the onset of alternans.

In closing, we remark that extending our results to the case of alternans may be quite challenging. If $\alpha > 1$, the operator T no longer has the property that $\|T^n \varphi\|_\infty \rightarrow 0$ as $n \rightarrow \infty$ for all $\varphi \in C[0, L]$. Thus, a similar analysis of the alternans regime would require a substantially different approach, which we hope to provide in a future study.

Appendix. Sample restitution and dispersion curves. For the purpose of numerical simulation, we provide sample formulas for restitution and dispersion curves (73) and (74) for a particular choice of parameters. Using asymptotics, such formulas can be derived [4, 20] from the equations of an idealized ionic model [17, 20]; we omit the details here. Below, we measure DI values in ms and we use the following parameters:

$$(69) \quad \begin{aligned} \tau_{\text{in}} &= 0.1 \text{ ms}, & \tau_{\text{out}} &= 2.4 \text{ ms}, & \tau_{\text{open}} &= 130 \text{ ms}, \\ \tau_{\text{close}} &= 150 \text{ ms}, & \kappa &= 10^{-3} \frac{\text{cm}^2}{\text{ms}}. \end{aligned}$$

Let

$$(70) \quad h(DI) = 1 - (1 - h_{\text{min}}) e^{-DI/\tau_{\text{open}}}$$

and

$$(71) \quad V_{\pm}(DI) = \frac{1}{2} \left(1 \pm \sqrt{1 - \frac{h_{\text{min}}}{h(DI)}} \right),$$

where

$$(72) \quad h_{\text{min}} = \frac{4\tau_{\text{in}}}{\tau_{\text{out}}}.$$

Note that $h(DI)$ and $V_{\pm}(DI)$ are dimensionless. In all numerical simulations, we use the restitution function

$$(73) \quad f(DI) = \tau_{\text{close}} \ln \left[\frac{h(DI)}{h_{\text{min}}} \right]$$

and the dispersion function

$$(74) \quad c(DI) = \max \left\{ \left[\frac{1}{2} V_+(DI) - V_-(DI) \right] \sqrt{\frac{2\kappa h(DI)}{\tau_{\text{in}}}}, 0 \right\}.$$

Note that $f(DI)$ has units of ms and $c(DI)$ has units of cm/ms.

REFERENCES

- [1] I. BANVILLE AND R. A. GRAY, *Effect of action potential duration and conduction velocity restitution and their spatial dispersion on alternans and the stability of arrhythmias*, J. Cardiovasc. Electrophysiol., 13 (2002), pp. 1141–1149.
- [2] M. R. BOYETT AND B. R. JEWELL, *A study of the factors responsible for rate-dependent shortening of the action potential in mammalian ventricular muscle*, J. Physiol., 285 (1978), pp. 359–380.
- [3] J. W. CAIN, *Issues in the One-Dimensional Dynamics of a Paced Cardiac Fiber*, Ph.D. dissertation, Duke University, Durham, NC, 2005.
- [4] J. W. CAIN, E. G. TOLKACHEVA, D. G. SCHAEFFER, AND D. J. GAUTHIER, *Rate-dependent propagation of cardiac action potentials in a one-dimensional fiber*, Phys. Rev. E (3), 70 (2004), pp. 061906.
- [5] J. CAO, Z. QU, Y. KIM, T. WU, A. GARFINKEL, J. N. WEISS, H. S. KARAGUEUZIAN, AND P. CHEN, *Spatiotemporal heterogeneity in the induction of ventricular fibrillation by rapid pacing: Importance of cardiac restitution properties*, Circ. Res., 84 (1999), pp. 1318–1331.
- [6] E. M. CHERRY AND F. H. FENTON, *Suppression of alternans and conduction blocks despite steep APD restitution: Electrotonic, memory, and conduction velocity restitution effects*, Am. J. Physiol., 286 (2004), pp. H2332–H2341.
- [7] M. COURTEMANCHE, L. GLASS, AND J. P. KEENER, *Instabilities of a propagating pulse in a ring of excitable media*, Phys. Rev. Lett., 70 (1993), pp. 2182–2184.
- [8] M. COURTEMANCHE, J. P. KEENER, AND L. GLASS, *A delay equation representation of pulse circulation on a ring in excitable media*, SIAM J. Appl. Math., 56 (1996), pp. 119–142.
- [9] E. CYTRYNBAUM AND J. P. KEENER, *Stability conditions for the traveling pulse: Modifying the restitution hypothesis*, Chaos, 12 (2002), pp. 788–799.
- [10] N. DUNFORD AND J. T. SCHWARTZ, *Linear Operators. Part I: General Theory*, Interscience, New York, 1958.
- [11] B. ECHEBARRIA AND A. KARMA, *Instability and spatiotemporal dynamics of alternans in paced cardiac tissue*, Phys. Rev. Lett., 88 (2002), pp. 208101.
- [12] J. J. FOX, R. F. GILMOUR, JR., AND E. BODENSCHATZ, *Conduction block in one dimensional heart fibers*, Phys. Rev. Lett., 89 (2002), pp. 198101–198104.
- [13] L. H. FRAME AND M. B. SIMSON, *Oscillations of conduction, action potential duration, and refractoriness*, Circulation, 78 (1988), pp. 1277–1287.
- [14] M. R. GUEVARA, G. WARD, A. SHRIER, AND L. GLASS, *Electrical alternans and period doubling bifurcations*, in Proceedings of the 11th Computers in Cardiology Conference, IEEE Computer Society, Los Angeles, 1984, pp. 167–170.
- [15] G. M. HALL, S. BAHAR, AND D. J. GAUTHIER, *Prevalence of rate-dependent behaviors in cardiac muscle*, Phys. Rev. Lett., 82 (1999), pp. 2995–2998.
- [16] H. ITO AND L. GLASS, *Theory of reentrant excitation in a ring of cardiac tissue*, Phys. D, 56 (1992), pp. 84–106.
- [17] A. KARMA, *Spiral breakup in model equations of action potential propagation in cardiac tissue*, Phys. Rev. Lett., 71 (1993), pp. 1103–1107.
- [18] J. P. KEENER, *Waves in excitable media*, SIAM J. Appl. Math., 39 (1980), pp. 528–548.
- [19] J. P. KEENER AND J. SNEYD, *Mathematical Physiology*, Springer-Verlag, New York, 1998.
- [20] C. C. MITCHELL AND D. G. SCHAEFFER, *A two-current model for the dynamics of cardiac membrane*, Bull. Math. Bio., 65 (2003), pp. 767–793.
- [21] G. R. MINES, *On dynamic equilibrium in the heart*, J. Physiol. (London), 46 (1913), pp. 349–383.
- [22] J. C. NEU, R. S. PREISSIG, JR., AND W. KRASSOWSKA, *Initiation of propagation in a one-dimensional excitable medium*, Phys. D, 102 (1997), pp. 285–299.
- [23] J. B. NOLASCO AND R. W. DAHLEN, *A graphic method for the study of alternation in cardiac action potentials*, J. Appl. Physiol., 25 (1968), pp. 191–196.
- [24] J. M. PASTORE, S. D. GIROUARD, K. R. LAURITA, F. G. AKAR, AND D. S. ROSENBAUM, *Mechanism linking T-wave alternans to the genesis of cardiac fibrillation*, Circulation, 99 (1999), pp. 1499–1507.
- [25] R. PLONSEY AND R. C. BARR, *Bioelectricity: A Quantitative Approach*, Plenum Press, New York, 1988.
- [26] M. REED AND B. SIMON, *Methods of Modern Mathematical Physics I: Functional Analysis*, Academic Press, San Diego, 1980.
- [27] J. RINZEL AND K. MAGINU, *Kinematic analysis of wave pattern formation in excitable media*, in Nonequilibrium Dynamics in Chemical Systems, A. Pacault and C. Vidal, eds., Springer-Verlag, Berlin, 1984, pp. 107–113.

- [28] D. S. ROSENBAUM, P. ALBRECHT, AND R. J. COHEN, *Predicting sudden cardiac death from T wave alternans of the surface electrocardiogram: Promise and pitfalls*, J. Cardiovasc. Electrophysiol., 7 (1996), pp. 1095–1111.
- [29] D. S. ROSENBAUM, L. E. JACKSON, J. M. SMITH, H. GARAN, J. N. RUSKIN, AND R. J. COHEN, *Electrical alternans and vulnerability to ventricular arrhythmias*, New Engl. J. Medicine, 330 (1994), pp. 235–241.
- [30] H. SEDAGHAT, C. M. KENT, AND M. A. WOOD, *Criteria for the convergence, oscillation, and bistability of pulse circulation in a ring of excitable media*, SIAM J. Appl. Math., 66 (2005), pp. 573–590.
- [31] S. STROGATZ, *Nonlinear Dynamics and Chaos*, Perseus, Cambridge, MA, 1994.
- [32] G. SZEGŐ, *Orthogonal Polynomials*, 4th ed., AMS, Providence, RI, 1975.
- [33] J. J. TYSON AND J. P. KEENER, *Singular perturbation theory of traveling waves in excitable media (a review)*, Phys. D, 32 (1988), pp. 327–361.
- [34] M. A. WATANABE, F. H. FENTON, S. J. EVANS, H. M. HASTINGS, AND A. KARMA, *Mechanisms for discordant alternans*, J. Cardiovasc. Electrophys., 12 (2001), pp. 196–206.
- [35] A. R. YEHA, D. JEANDUPEUX, F. ALONSO, AND M. R. GUEVARA, *Hysteresis and bistability in the direct transition from 1:1 to 2:1 rhythm in periodically driven single ventricular cells*, Chaos, 9 (1999), pp. 916–931.